AUTOMOBILE STRUCTURAL HEALTH MONITORING PERFORMED USING LONG PERIOD GRATING FIBER SENSORS

Dan SAVASTRU[1], Sorin MICLOS[2], Roxana SAVASTRU[3], Florina-Gianina ELFARRA[4], Ion LANCRANJAN[5]

Structural Health Monitoring (SHM) is important for instantly and continuously diagnosis of the different parts and/or full assembly constituent materials "status" of an automotive structure. Automobile structure incorporate a large amount of parts manufactured of composite materials. The paper aims to present how SHM can be performed using Long Period Grating Fiber Sensors (LPGFS). SHM means to observe in-situ two main types of automobile structure parameters: physical (mechanical) and/or chemical. LPGFS can be used as embedded in polymer matrix of composite materials or applied on composite parts of automobile structure as economically effective mechanical and/or chemical sensors.

Keywords: Structural Health Monitoring, Long Period Grating, Fiber Optics.

1. Introduction

During the last decades, as in aeronautical applications, in automotive industry the structural reliability and operational health monitoring have become increasingly important in conjunction with a change of the philosophy of safe-life over the fail-safe approaches in the design of metallic as well as composite structures [1-10].

The main purpose of the work is to present the development of an innovative system for Structural Health Monitoring (SHM) of automotive structures into which many parts are manufactured of composite materials. The developed SHM system is based on dynamic strain measurements for identifying in an exhaustive way the structural state condition. Long Period Grating Fiber Sensors (LPGFS) embedded into the polymer matrix of the composite materials are optical primary sensors used for dynamic strain measurements of the investigated automotive composite structure [11-20]. The primary data obtained from LPGFS are analyzed using a methodology allowing structural damage detection based on a statistical data-driven learning model, i.e. an artificial neural network, coupled with wavelet multi-resolution analysis [1-10]. This methodology is the core of the SHM system. To be more precise, the present work presents the first basic stage of the SHM system, namely how LPGFS is operated and how optical signals generated by this type of sensors can be correlated with what is happening in the observed

automotive structure namely various thermal and mechanical loads such as strain, torsion, elongation and compression. The presented results are closely related to the concept of Smart Polymer Composite Materials (SPCM) [11-20].

It is interesting to analyze how necessity of improved automotive design led to the presented SHM system. Over the last years the attention began to be focused on smart structures with inherent sensing capabilities. For direction dynamic strain measurements using Fiber Bragg Grating (FBG) sensors for vibration-based structural health monitoring especially in composite structures is a quite promising technique [1]. The FBGs can be integrated into the material or fixed as patches on the surface. In general, fiber optic sensors have proved a reliable strain measuring capability combined with mechanical characteristics such as light weight, small size and immunity to electromagnetic interference [11]. FBGs offer multiplexing capabilities [11-13]. FBGs can be placed in great number at predetermined locations on the same Single Mode (SM) optical fiber as an array of quasi-distributed sensors that can be multiplexed [2]. LPGFSs have emerged on the optical fiber sensors in the last years. Compared to FBGs, LPGFSs have the advantage that they can be operated as mechanical and/or chemical sensors [21-25]. It is worth to underline the fact that, if necessary, by their structure, like the FBGs but with much more efficient designs, the LPGFSs can be also manufactured on SM optical fiber [21-25]. For both FBGs and LPGFS, proper designs of SHM systems into which are mounted is essential. For accomplishing such proper designs accurate simulation of FBGs and LPGFSs operation is vital. This paper presents results obtained in simulation of LPGFSs embedded into polymer matrix of composite materials [15-21].

2. Paper contents

In Fig. 1 there is presented schematically the structure of a LPGFS and how it works. A LPGFS is manufactured into a SM optic fiber by inducing a permanent spatial modulation of the light propagation characteristics over a length L. The permanent spatial modulation represents an equivalent periodic perturbation of n_{core}, the SM optic fiber core refractive index, typically with a period of between 1 μm and 1000 μm. A diffraction grating denoted as Long Period Grating (LPG) is formed. LPG causes light to be coupled from the fundamental mode guided through the SM optical fiber core to a discrete set of cladding light copropagating modes for which the Bragg resonance condition if fulfilled [10-15]. It is necessary to emphasize that the term copropagating modes refers to light propagation in the same sense. The SM optical fiber zone where the LPG is manufactured is stripped of the PMMA mechanical protection layer. Therefore, the SM optic fiber cladding is in direct contact with the ambient into which the LPGFS is mounted. This LPGFS constructive characteristic is very important for their use as chemical sensors. For comparison, an FBG is also a periodic modulation of n_{core} but with a period of

several hundreds of nanometers (400-600 nm) in an optical fiber which has the PMMA mechanical protection layer. Thus, the grating is isolated from the ambient.

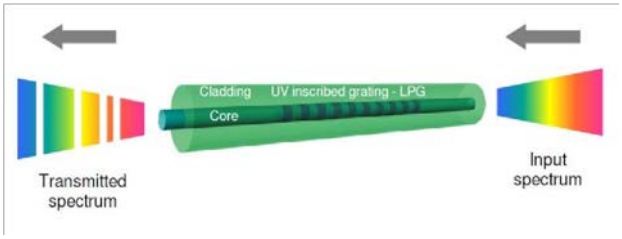

Fig. 1. Schematic representation of a LPGFS and its operation mode [12].

In Fig. 1 it can be observed how a LPGFS is operated. The input light beam emitted by a source with an "Input spectrum" propagates guided through the SM optical fiber core as the fundamental mode is diffracted by the LPG on which is incident at blazing angle. An LPG acts as an optical fiber-based grating that enables coupling between the core and the cladding co-propagation modes. This coupling between propagation modes represents an electromagnetic energy transfer from the core mode to the possible cladding modes [15-19]. The transferred energy is lost from the fundamental light mode and can continue its propagation through the cladding until it is lost into the ambient, kept into core proximity volume or coupled back, when meeting another LPG, to the fundamental mode. This energy transfer is maximum at discrete wavelengths λ^i defined by the Bragg resonance condition [11-17]

$$\lambda^i = \left(n_{eff} - n_{clad}^i \right) \cdot \Lambda \tag{1}$$

where λ^i is the central wavelength of the absorption band observed in the LPGFS transmission spectrum, n_{eff} is the refractive index effective value of the i^{th} possible cladding propagation mode and Λ is the period of the LPG. Equation (1) is useful for sensing observing that the effective values of refractive index of core and cladding propagation modes depend on ambient refractive index [11-16]. Any infinitesimal modification of the ambient refractive index represents a change in characteristics of light propagation through the LPGFS and is sensed by the LPG by observing the spectral shifting and broadening of each absorption bands induced in SM optic fiber transmission spectrum [11-25]. In the FBGs case because the mode coupling caused by the grating between light propagation modes take place only between the fundamental mode and counter-propagating ones, a fact imposed by energy and impulse conservation laws, the single modification of the light spectrum will consist of one sharp reflection band centered at λ_B, the Bragg wavelength [11-15].

A SHM system must observe simultaneously several parameters connected to automotive motion or aircraft flight, among which vibrations types (longitudinal or transversal), frequency and amplitude are very important one [1-10]. This is equivalent to change from the common static analyses made on SM optic fiber sensitivities to a dynamical one. Dynamic influences on physical parameter such as mechanical vibrations should be considered in practice. When a vibration in an axial direction occurs somewhere in the SM optic fiber ambient, the deformation will propagate along the fiber to form a longitudinal mechanical wave in its axial direction. Because the fiber is very thin compared to its length and its transverse deformation can occur freely in case of no external force applied on the circumference, the propagation equation is written as [18].

$$\rho \frac{\partial^2 u_z}{\partial t^2} = Y \frac{\partial^2 u_z}{\partial z^2} \tag{2}$$

In Eq. (1) ρ is the fiber optic density, Y is the Young's module and u_z is a displacement transverse to z axis. The transverse vibration wave u_z means a bending wave along the optical fiber [18-25]. Regarding the LPGFS operation, the transverse vibration wave propagating along the SM optical fiber which will be observed as spectral shifting and broadening of each absorption bands existing in SM optical fiber transmission spectrum [11-25].

3. Simulation Results

As mentioned in Section 2, the simulation of the smart was performed in several steps. The simulation was performed using the three layers model of the optic fiber, i.e. core, cladding and ambient. The simulation was performed considering the case of Fibercore SM750 optical fiber, which is, according to literature, commonly used as host for LPG. In Table 1 the parameters of the optical fiber and of the LPG considered as input data for simulation are presented. The simulation was performed considering that λ, the light propagation wavelength, is situated in the spectral domain 700 - 1700 nm. The first step of the simulation consists in calculating the core effective refraction index, n_{effco}, variation with the light propagation wavelength. This task was accomplished by solving the dispersion equation using the bisection method. The second step consists in calculation of cladding refractive effective refractive index variation with λ for several possible propagation modes LP_{0i}. There were considered only such possible clad propagation modes for which the coupling with the core single mode propagation is significant, meaning large values of coupling coefficient. The presented results were obtained considering the first nine such possible clad propagation modes. The simulation was accomplished for different values of ambient refractive index, i.e. air (for calibrating LPGFS) and several common polymers used for composite materials manufacturing.

Table 1

Parameters of the optical fibre and of LPG.

Parameter	Value	Parameter	Value
Core radius	2.8 μm	Core ref. ind.	1.458
Clad radius	62.5 μm	Clad ref. ind.	1.454
Cut-off wlen.	650 nm	Amb. ref. ind.	1.000
LPG period	400–800 μm	LPG length	1 - 100 mm

In Table 2 the lower (λ_{lower}) and upper (λ_{upper}) values of wavelength of guided light propagating through the SM optic fiber core are indicated for the investigated polymers. The LPGFS operation procedure is strongly related to these spectral domains in the sense that for a given wavelength of the guided light and grating period there are obtained the peaks of the LPG absorption bands corresponding to cladding propagation modes.

Table2

Characteristics of the polymers used for the composite matrix

Polymer	Acronym	Chemical formula	Refractive index	λ_{lower} [nm]	λ_{upper} [nm]
Polyvinyl alcohol	PVA	$(C_2H_4O)_n$	1.4839	450	600
Polylactic acid	PLA	$(C_3H_4O_2)_n$	1.4589	450	600
Polymethylmethacrylate	PMMA	$(C_5H_8O_2)_n$	1.4906	500	1000
Polyvinylpyrrolidone	PVP	$(C_6H_9NO)_n$	1.5274	400	900
Cellulose		$(C_6H_{10}O_5)_n$	1.4701	500	1000
Polystyrene	PS	$(C_8H_8)_n$	1.5916	500	1000
Polycarbonate	PC	$(C_{16}H_{14}O_3)_n$	1.5848	500	1000

In Table 3 there are presented some of the simulation results obtained for the first ten cladding propagation modes in the cases of investigated polymers considering a grating period of 600 μm and a grating length of 50 mm. The term “first nine” refers to the cladding modes which propagate into a volume in the proximity of the core. For this kind of cladding propagating modes, the coupling with the core fundamental mode has the highest values. In Table 3 there can be noticed for each of the investigated polymers, considering an incident light having a wavelength of 800 nm, the values obtained for absorption bands peaks, denoted as λ^i, and bandwidths, denoted as $\Delta\lambda$.

Table3

Simulation results for the LPGFS resonance absorption bands peak wavelengths and FWHM bandwidth

Clad mode	Parameter	Polymer						
		PVA	PLA	PMMA	PVP	Cellulose	PS	PC
# 1	λ^i [μm]	0.859	0.857	0.857	0.858	0.857	0.859	0.857
	Δλ [nm]	5.9	5.8	5.8	5.9	5.8	5.9	5.9
# 2	λ^i [μm]	0.864	0.864	0.864	0.864	0.864	0.864	0.864
	Δλ [nm]	6.0	6.0	6.0	6.0	6.0	6.0	6.0
# 3	λ^i [μm]	0.868	0.868	0.868	0.868	0.868	0.868	0.868
	Δλ [nm]	6.2	6.2	6.1	6.3	6.2	6.2	6.2
# 4	λ^i [μm]	0.873	0.873	0.873	0.873	0.873	0.873	0.873
	Δλ [nm]	6.5	6.4	6.5	6.6	6.6	6.6	6.5
# 5	λ^i [μm]	0.881	0.881	0.881	0.881	0.881	0.881	0.881
	Δλ [nm]	7.1	7.0	7.1	7.1	7.2	7.1	7.1
# 6	λ^i [μm]	0.890	0.890	0.890	0.890	0.890	0.890	0.890
	Δλ [nm]	7.8	7.8	7.8	7.8	7.8	7.8	7.8
# 7	λ^i [μm]	0.903	0.903	0.903	0.903	0.903	0.903	0.905
	Δλ [nm]	8.3	8.3	8.3	8.3	8.3	8.3	8.4
# 8	λ^i [μm]	0.916	0.918	0.917	0.917	0.916	0.917	0.918
	Δλ [nm]	8.7	8.7	8.6	8.7	8.7	8.8	8.7
# 9	λ^i [μm]	0.938	0.938	0.938	0.938	0.938	0.938	0.939
	Δλ [nm]	9.2	9.2	9.4	9.2	9.2	9.4	9.3
# 10	λ^i [μm]	0.957	0.962	0.960	0.963	0.961	0.960	0.962
	Δλ [nm]	9.8	9.8	9.8	9.8	9.8	9.9	9.9

In Fig. 2a there are presented the results obtained in simulating the variations of effective values of core and cladding refractive index with wavelength of light propagating through the optic fiber core incident on the LPG considering air as ambient. In Fig. 2b, for the first ten cladding propagation modes, there are presented the results obtained in simulating the phase matching curves for the investigated LPGFS using Eq. (1) in the case of ambient air.

The key of LPGFS operation modes becomes clear after analyzing the significance of the phase matching curves. In Fig. 2b it can be observed that phase matching curves are parametric curves defined into domains of LPG grating period, Λ_{LPG}, and guided light wavelength. The following procedure is quite simple: imagine a horizontal or vertical line, i.e. corresponding to a given value of Λ_{LPG} or light wavelength; the intersection points of this horizontal or vertical line with the phase matching curves defines the peaks λ^i of absorption bands appearing the optic fiber transmission spectrum. In common cases, for a given Λ_{LPG}, at a wavelength of the emission spectrum of a light source coupled to the LPGFS, corresponds

several absorption bands each of them being induced by energy transfer to a cladding propagation mode.

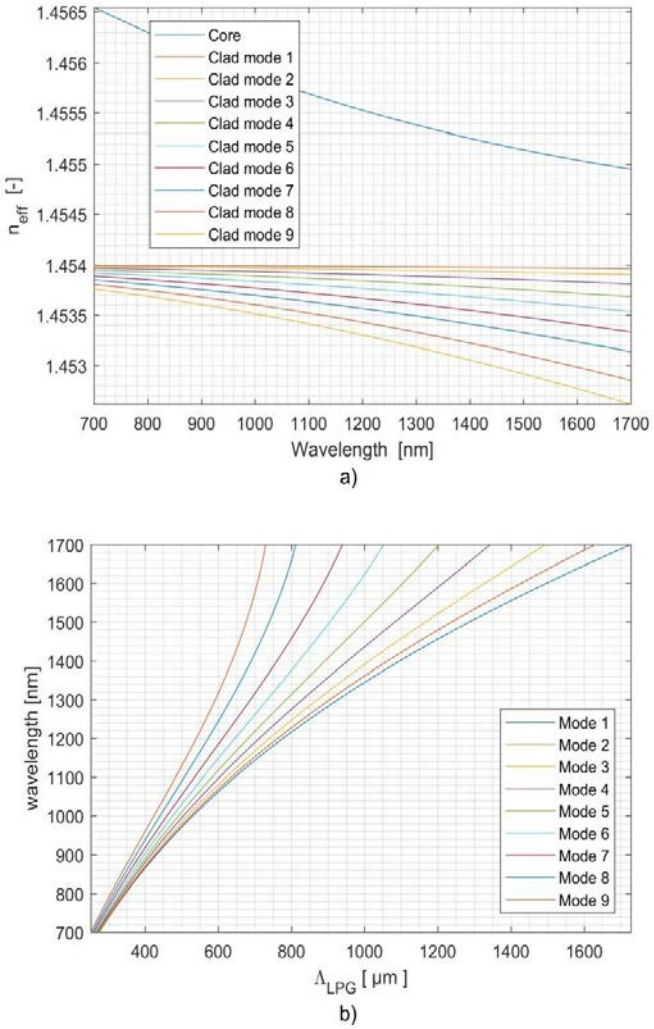

Fig. 2. The variations with wavelength of effective refractive index for core and the first nine cladding modes (a) and of wavelength with Λ_{LPG} calculated for the first nine cladding modes (b).

In Fig. 3 there are presented the variations of effective values of refractive index corresponding to cladding propagation modes simulated for several of the polymers denominated in Table 2.

This is the starting point in the sense that for a polymer of Table 2, by repeating the procedure defined by Fig. 2 b, it is possible to obtain λ^i.

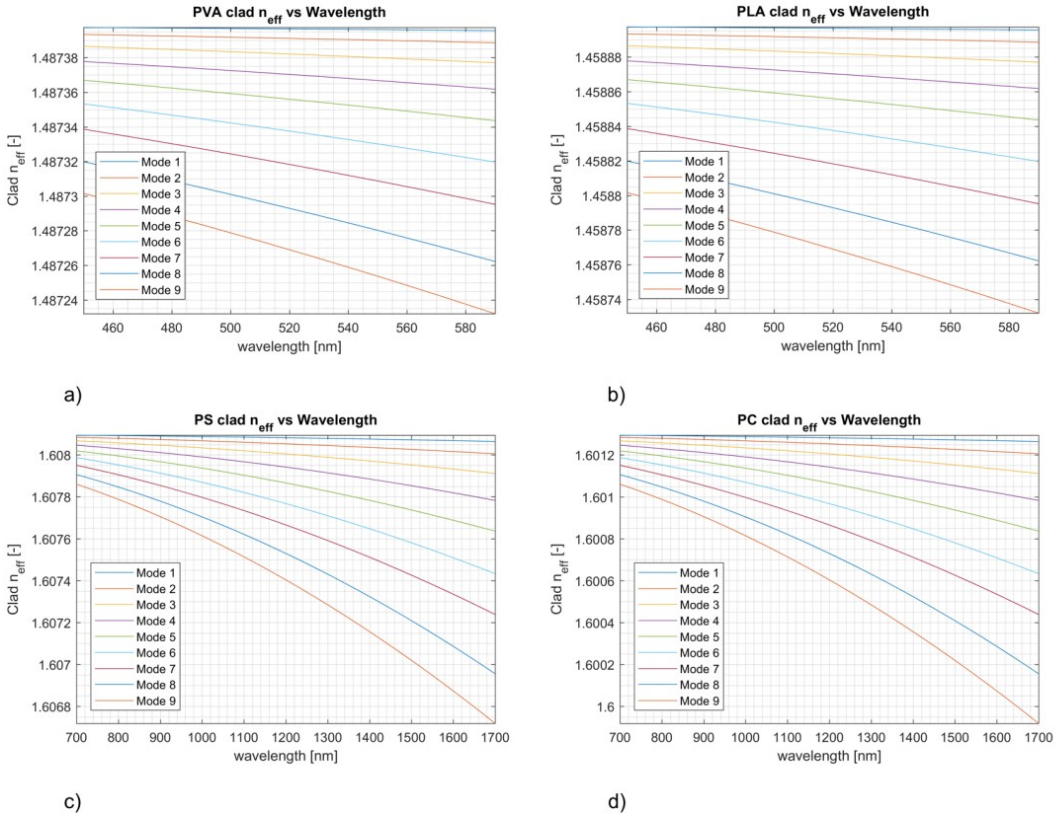

Fig. 3. The calculated effective refractive index (n_{effcl}) of cladding propagating modes variation with wavelength for PVA (a), PLA (b), PS (c) and PC (d).

By observing variations of λ^i induced by changes of ambient refractive index alteration or by LPGFS mechanical and geometrical modifications it is possible the LPGFS operation. The sensing mechanism appears at a first glance as complicated, but it can be efficient because for a given Λ_{LPG} there is obtained a set of λ^i each corresponding to a cladding propagation mode.

Each λ^i is the wavelength of a peak of an absorption band. Each such absorption band has a bandwidth which varies with the order of cladding propagation mode order. This a second kind of information useful for sensing operation. The third kind of information eventually useful for sensing is related to spectral splitting of the Bragg resonance absorption bands induced by the ambient into the LPGFS transmission spectrum. This third kind of information is related to polarization effects induced by the ambient in the optical fiber and measured by the amplitude of the spectral splitting between the two peaks.

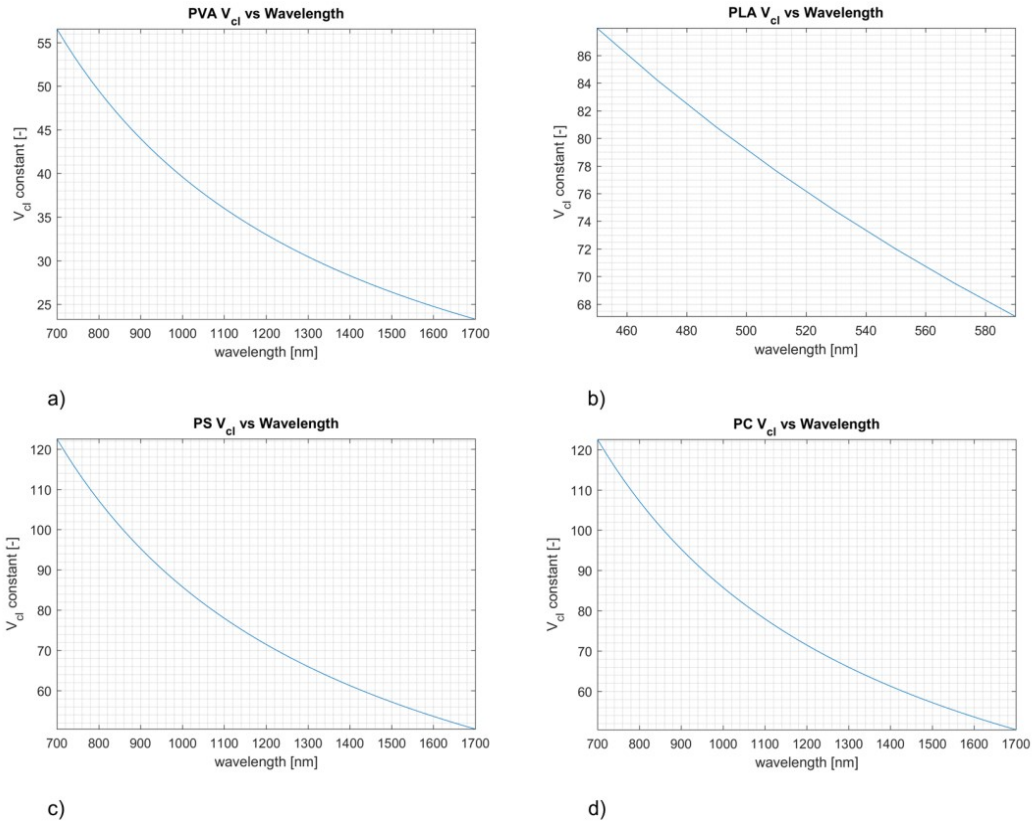

Fig. 4. The calculated V-number of the cladding (Vcl) for PVA (a), PLA (b), PS (c) and PC (d).

The simulation results presented in Figs. 2, 3 and 4 constitute the first stages of design of SHM systems based on LPGFS embedded in polymer matrix of composite materials. As previously mentioned, operation of a SHM system basically relies on measuring/monitoring simultaneously several parameters which can be connected to automotive motion or aircraft flight, mainly by inherent vibrations. For sensing operation, the type of structure vibration, longitudinal or transversal, is important. Depending on the effective structure design and the place in the structure where is mounted the part made of composite material into whose polymer matrix is embedded the LPGFS, any spectral shift and broadening of the Bragg resonance absorption band is an important information. The amplitude of λ^i displacement gives the magnitude of vibration effects on the health of the structure. The time response of LPGFS is five to ten orders of magnitude than the characteristic times of mechanical vibrations of the investigated structure. This is important for real time measurements. An important observation concerning SHM performed using LPGFS refers to the “static point” of the automobile or aircraft structure. The LPGFS have no remanence. This means that if after the automotive

motion or aircraft flight stop, when it is stationary, there are not any observable λ^i displacement and/or broadening of the corresponding absorption band, the net result concerning SHM is positive in the sense that the structure is in the same status. This means that frequency and amplitude of structure vibrations are kept in the operational domains [1-10]. This is equivalent to change from the common static analyses made on SM optic fiber sensitivities to a dynamical one and back. Dynamic influences on physical parameter such as mechanical vibrations should be considered in practice by observing λ^i displacements and/or absorption band broadening.

6. Conclusions

For development of a software package dedicated for automobile SHM, an optical LPGFS manufactured in a given commercial optic fiber and embedded into different types of polymers used as matrix for composite materials was simulated. The numerical results obtained in calculations of core and clad effective refractive indexes variations over an extended propagation wavelength range were used as a starting point of the composite properties simulation process. On this basis, for a given LPG period, there were calculated resonance wavelengths characteristics for several cladding propagation modes. The results obtained in calculation of coupling coefficients of core and clad radiation modes, followed by the ones obtained in evaluation of absorption coefficients are presented as the simulation next stages. As the final two stages, the transmission spectra, the shift and the bandwidth broadening specific for a resonant wavelength, both induced by a bending deformation of optic fiber, are presented as calculated by using the developed software design package. The simulation results are in good agreement with experimental ones reported in literature [12-19]. In this sense, the software design package proves to be useful for calculation of core and clad refractive indexes variations with propagation wavelength, long period grating resonance wavelengths as depending on its period, the absorption coefficients at these resonance wavelengths and consequently, of its transmission spectra.

Acknowledgment

This research is supported by MANUNET grant MNET17/ NMCS0042 and by the Core Program project no. PN 18 28.01.01.

R E F E R E N C E S

[1]. *W. Staszewski, C. Boller, G. Tomlinson*, Health Monitoring of Aerospace Structures: Smart sensor technology and signal processing, John Wiley & Sons Inc., Chichester, England, 2004.

[2]. *J. R. Dunphy, G. Meltz, W. W. Morey*, Optical Fiber Bragg Grating Sensors: A candidate for Smart Structures Application. In *E. Udd* ed., Fiber Optic Smart Structures, John Wiley & Sons Inc., NY, 1995.

[3]. *P. Capoluongo, C. Ambrosino, S. Campopiano, A. Cutolo, M. Giordano, I. Bovio, L. Lecce, A. Cusano*, "Modal analysis and damage detection by Fiber Bragg grating sensors", in Sensor Actuator, **vol. 133**, no. 2, Feb. 2007, pp. 415-424.

[4]. *A. Paolozzi, P. Gasbarri*, "Dynamic analysis with fibre optic sensors for structural health monitoring, multifunctional structures/integration of sensors and antennas", in Meeting proceedings RTO-MP-AVT-141, paper 9, Neuilly-sur-Seine, France: RTO, 2009, pp. 9.19.24.

[5]. *L. Sun, H. Li, L. Ren, Q. Jin*, "Dynamic response measurement of offshore platform model by FBG sensors", in Sensor Actuat A-Phys, **vol. 136**, no. 2, May 2007, pp. 572-579.

[6]. *A. Shimada, K. Urabe, Y. Kikushima, J. Takahashi, K. Kageyama*, "Detection of Missing Fastener Based on Vibration Mode Analysis Using Fiber Bragg Grating (FBG) Sensors", Proc SPIE, **vol. 5056**, Aug. 2003, pp. 312-318.

[7]. *S. Takeda, Y. Aoki, T. Ishikawa, N. Takeda, H. Kikukawa*, "Structural health monitoring of composite wing structure during durability test", in Compos Struct, **vol. 79**, no. 1, Jun. 2007, pp. 133-139.

[8]. *J. A. Güemes, J. M. Menendez, M. Frövel, I. Fernandez, J. M. Pintado*, "Experimental analysis of buckling in aircraft skin panels by fibre optic sensors", in Smart Mater Struct, **vol. 10**, no. 3, 2001, pp. 490-496.

[9]. *M. Mieloszyk, M. Krawczuk, A. Zak, W. Ostachowicz*, "An adaptive wing for a small-aircraft application with a configuration of fibre Bragg grating sensors", in Smart Mater Struct, **vol. 19**, no. 8, 2010, pp. 1-12.

[10]. *K. Dragran, P. Klimaszewski, P. Kudela, P. Malinowski, T. Wandowski*, "Health Monitoring of the helicopter main rotor blades with the structure integrated sensors", in Procs Fifth European Workshop of Structural Health Monitoring, 2010, pp. 63-69.

[11]. *M. Dvorak, M. Ruzicka, V. Kulisek, J. Behal, V. Kafka*, "Damage Detection of the Adhesive Layer of Skin Doubler Specimens Using SHM System Based on Fiber Bragg Gratings", in Procs Fifth European Workshop of Structural Health Monitoring, 2010, pp. 70-75.

[12]. *S. W. James, R. P. Tatam*, "Optical fibre long-period grating sensors: characteristics and application", in Meas Sci Technol, **vol. 14**, 2003, pp. R49-R61.

[13]. *A. M. Vengsarkar, P. J. Lemaire, J. B. Judkins, V. Bhatia, T. Erdogan, J. E. Sipe*, "Long Period Fiber Gratings as Band Rejection Filters", in J Lightwave Technol, **vol. 14**, no. 1, 1996, pp. 58-65.

[14]. *T. Erdogan*, "Cladding-mode resonances in short- and long-period fiber grating filters", in J Opt Soc Am A, **vol. 14**, no. 8, 1997, pp. 1760-1773.

[15]. *T. Erdogan*, "Fiber grating spectra", in J Lightwave Technol, **vol. 15**, no. 8, Aug 1997, pp. 1277-1294.

[16]. *A. I. Kalachev, V. Pureur, D. N. Nikogosyan*, "Investigation of long-period fiber gratings induced by high-intensity femtosecond UV laser pulses", in Opt Commun, **vol. 246**, 2005, pp. 107–115.

[17]. *C. S. Cheung, S. M. Topliss, S. W. James, R. P. Tatam*, "Response of fiber-optic long-period gratings operating near the phase-matching turning point to the deposition of nanostructured coatings", in J Opt Soc Am B, **vol. 25**, no. 6, 2008, 897-902.

[18]. *L. Zhang, W. Zhang, I. Bennion*, In-Fiber Grating Optic Sensors. In *S. Yin, P. B. Ruffin, F. T. S. Yu* ed. Fiber Optic Sensors, CRC Press, Boca Raton, FL, 2008.

[19]. *W. J. Bock, J. Chen, P. Mikulic, T. Eftimov*, "A novel fiber-optic tapered long-period grating sensor for pressure monitoring", in IEEE T Instrum Meas, **vol. 56**, Aug. 2007, pp. 1176–1180.

[20]. *D. Savastru, S. Miclos, R. Savastru, I. Lancranjan*, "Numerical Analysis of a Smart Composite Material Mechanical Component Using an Embedded Long Period Grating Fiber Sensor", in Proc SPIE, **vol. 9517**, 95172A, 2015.
[21]. *S. Miclos, D. Savastru, R. Savastru, I. Lancranjan*, "Numerical analysis of Long Period Grating Fibre Sensor operational characteristics as embedded in polymer", in Compos Struct, vol. **183**, no. SI, 2018, pp. 521-526.
[22]. *D. Savastru, S. Miclos, R. Savastru, I. Lancranjan*, "Study of thermo-mechanical characteristics of polymer composite materials with embedded optical fibre", in Compos Struct, vol. **183**, no. SI, 2018, pp. 682-687.
[23]. *E. Anemogiannis, E. N. Glytsis, T. K. Gaylord*, "Transmission Characteristics of LongPeriod Fiber Gratings Having Arbitrary Azimuthal/Radial Refractive Index Variations", in J Lightwave Technol, **vol. 21**, no. 1, Jan. 2003, 218-227.
[24]. *S. Khaliq, S. W. James, R. P. Tatam*, "Fiber-optic liquid-level sensor using a long-period grating", in Opt Lett, **vol. 26**, no. 16, 2001, pp. 1224-1226.
[25]. *K. O. Hill, B. Malo, F. Bilodeau, D. C. Johnson*, "Photosensitivity in Optical Fibers", in Annu Rev Mater Sci, **vol. 23**, Aug. 1993, pp. 125-157.
[26]. *S. Miclos, D. Savastru, I. Lancranjan*, "Numerical Simulation of a Fiber Laser Bending Sensitivity", in Rom Rep Phys, **vol. 62**, no. 3, 2010, pp. 519-527.
[27]. *I. Lancranjan, S. Miclos, D. Savastru*, "Numerical simulation of a DFB-fiber laser sensor (I)", in J Optoelectron Adv M, **vol. 12**, no. 8, Aug. 2010, pp. 1636-1645.
[28]. *I. Lancranjan, S. Miclos, D. Savastru, A. Popescu*, "Numerical simulation of a DFB-fiber laser sensor (II) - theoretical analysis of an acoustic sensor", in J Optoelectron Adv M, **vol. 12**, no. 12, Dec. 2010, pp. 2456-2461.
[29]. *R. Savastru, I. Lancranjan, D. Savastru, S. Miclos*, "Numerical simulation of distributed feed-back fiber laser sensors", in Proc SPIE, **vol. 8882**, 88820Y, 2013.
[30]. *S. Miclos, D. Savastru, R. Savastru, I. Lancranjan*, "Design of a Smart Superstructure FBG Torsion Sensor", in Proc SPIE, vol. **9517**, 95172B, 2015.
[31]. *D. Savastru, S. Miclos, R. Savastru, I. Lancranjan*, "Analysis of optical microfiber thermal processes", in Rom Rep Phys, **vol. 67**, no. 4, 2015, pp. 1586-1596.